Random Three-Dimensional Tilings of Aztec Octahedra and Tetrahedra: An Extension of Domino Tilings

Dana Randall* Gary Yngve†

Abstract

We present an extension of domino tilings of planar lattice regions to three dimensions. The tilings consist of filling "Aztec" octahedral and tetrahedral regions with triangular prisms. The set of tilings corresponds bijectively to a set of ordered domino tilings of planar regions, where the domino tilings are forced to respect a partial order based on a height function representation. We define a natural Markov chain on the set of tilings and prove that it is rapidly mixing. This is the first nontrivial proof of rapid mixing for a Markov chain on configurations which correspond to a 4-dimensional height function. Simulations based on this Markov chain have shown that a class of octahedral and tetrahedral regions will have frozen regions akin to the arctic circle theorem, which states that the nonfrozen regions of random tilings of the Aztec diamond converge to a circle. Next, we show that for a second class of tilings, the octahedral and tetrahedral tilings will have equal entropy. This is surprising because they correspond to ordered tilings of square and Aztec diamond regions, respectively, which are known to have different entropy in two dimensions.

1 Introduction.

Domino tilings of regions in $\mathbf{Z}^2$ have provided an amusing playground for combinatorialists, computer scientists and physicists for many years. The problem of counting tilings of square regions was first proposed by Fowler and Rushbrooke in 1937 [6] in the context of analyzing the thermodynamics of a 2-dimensional dimer system. This counting question was resolved in the early 1960's by Kasteleyn, Fisher and Temperley [9, 16] using an elegant algorithm based on evaluating Pfaffians. For a survey of the dimer model, see [7]. In the early 1990's a new flurry of activity started with a paper of Thurston [17], who defined a "height function" representation for tilings, and a paper of Elkies, Kuperberg, Larson and Propp [5], who introduced the Aztec diamond and found new methods for generating and counting tilings of these regions. (The Aztec diamond is defined as a region in $\mathbf{Z}^2$ with $\{2, 4, ..n-2, n, n, n-2, ..., 2\}$ squares on successive rows, each centered around the y axis.) It was later found that random tilings of Aztec diamonds have "frozen regions" that are predictably tiled, and that the unfrozen parts of the tilings converge to a circular shape, the so-called "arctic circle theorem" [8]. In contrast, the square region is known to be of maximum entropy, so no such phenomena would appear in its random tilings. Efficient methods have since been developed to produce random tilings of any simply connected region in $\mathbf{Z}^2$ based on a height function representation of the set of tilings [13, 14].

Given this explosion of activity, it is quite natural to consider 3-dimensional tilings. The story here has been less satisfying. There has been progress in enumerative combinatorics for bounding the number of tilings of cubic regions with $2 \times 1 \times 1$ "bricks" (see, e.g., [2]), and there is a method for algorithmically approximately counting and sampling such tilings [10]. Unfortunately, however, many of the underlying properties that have attracted combinatorialists have failed to generalize. In particular, there no longer seems to be a height function representation of these tilings, and proposed Markov chains based on local moves no longer connect the state space. Properties also fail to generalize to tilings with $2 \times 2 \times 1$ "slabs," which has also been proposed.

In this paper, we abandon the original physical motivation of modeling dimer systems and succeed in defining a natural 3-dimensional generalization of the domino tiling problem that *does* inherit the algebraic and combinatorial properties that have attracted so much attention. The tilings have a height function that maps each tiling to a surface in $\mathbf{Z}^4$. There is a bijection between the set of 3-dimensional tilings with "domino chains" $T_1 \preceq T_2 \preceq ... \preceq T_n$, where $\preceq$ refers to the partial order on domino tilings defined by the original height function. In addition, there is a simple Markov chain based on local moves that is ergodic and connects

*College of Computing and School of Mathematics, Georgia Institute of Technology, Atlanta GA 30332-0280, randall@math.gatech.edu. Research supported in part by NSF Career Grant No. CCR-9703206.

†College of Computing, Atlanta GA 30332-0280, gary@cc.gatech.edu

the state space. This has allowed us to examine typical tilings, and we have found surprising "arctic-circle-like" phenomena demonstrating frozen regions.

The innovation comes from tiling regions with triangular prisms, each having two $30°, 30°, 120°$ triangles and a square face connecting the long edges of the triangles. The tile was derived from a Levitov block, which consists of two of these prisms glued together along their square faces (although specifying the angles as we do here was not important) [11]. Levitov blocks have been a useful tool for demonstrating the height function representation of 2-dimensional tilings. We define four interesting families of regions to be tiled, $\mathcal{O}_n, \mathcal{T}_n, \widehat{\mathcal{O}}_n$ and $\widehat{\mathcal{T}}_n$, where regions $\mathcal{O}_n$ and $\widehat{\mathcal{O}}_n$ are octahedral in shape and are defined from the height function of the 2-dimensional square region of order n, and $\mathcal{T}_n$ and $\widehat{\mathcal{T}}_n$ are tetrahedral in shape and are derived from the 2-dimensional Aztec diamond of order $n/2$.

The first result is that the natural Markov chain on the state space of tilings is rapidly mixing. The proof relies on path coupling and an intermediate step whereby we first analyze a Markov chain enhanced with "tower moves." This is the first proof of rapid mixing for a model represented by a 4-dimensional height function.

Simulating this Markov chain has allowed us to make several conjectures about emerging regions which are analogous to the 2-dimensional arctic circle theorem. We believe that regions $\mathcal{O}_n$ and $\mathcal{T}_n$ have frozen regions with predictable tilings when n is large.

The second result identifies a surprising connection between the Aztec diamond and the square region and allows us to prove that the entropy of tilings of $\widehat{\mathcal{O}}_n$ is *equal* to the entropy of tilings of $\widehat{\mathcal{T}}_n$. (The entropy is defined as $\lim \log(\#R_n)/\mathrm{Vol}(R_n)$, where R_n is a family of regions and $\#R_n$ is the number of tilings.) In two dimensions, tilings of the square and the Aztec diamond are known to have different entropy. The proof relies on a cute combinatorial identity that decomposes squares and Aztec diamonds into exact packings of smaller squares and diamonds.

The paper is organized as follows. We provide a very brief introduction into the theory of height functions in section 2. In section 3 we introduce the new tilings model. In section 4 we review the analysis of a Markov chain for sampling domino tilings. Then we define a Markov chain on the state space of 3-dimensional prism tilings and show that this is rapidly mixing. Finally, in section 5 we study random tilings of these regions. In particular, we prove that the octahedral and tetrahedral pyramids $\widehat{\mathcal{O}}$ and $\widehat{\mathcal{T}}$ have the same entropy. In addition, we show simulations that suggest there will be frozen regions that emerge almost surely in some random tilings.

2 Domino tilings and height functions.

A domino tiling is a covering of a finite, simply connected region of the Cartesian lattice with unmarked dominoes, where each domino covers two adjacent squares of the region. Domino tilings represent configurations of dimer systems on this lattice.

The tilings of any region can be represented by a height function. The height function arises from an underlying tiling group and can be summarized using a rule based on the bipartition underlying the dual lattice, i.e., the black and white squares of the chessboard. To define the height function h_T associated with a tiling T, start with some point v on the boundary and set $h_T(v) = 0$. Now, walking along edges bounding the tiles, if the square to the left of an edge is black (respectively, white), increase (respectively, decrease) the height by one. An example is illustrated in figure 1. It is easy to see that the height of a point on any tiling of a region is always fixed mod 4. Altering a tiling by "rotating" two adjacent horizontal tiles so that they are vertical (or vice-versa) alters the height function by changing the height of the center point by ± 4.

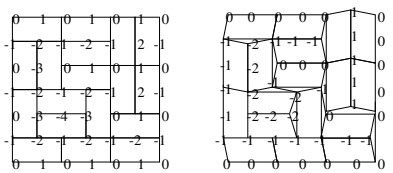

Figure 1: Domino tilings and height functions

This height function defines a partial order on tilings. We say that $T_1 \preceq T_2$ if, for each point p in the region, $h_{T_1}(p) \leq h_{T_2}(p)$. Every finite, simply connected region has a unique highest and lowest tiling. The highest and lowest tilings of the square and Aztec diamond are shown in figure 2; to see the associated height functions, see figure 5.

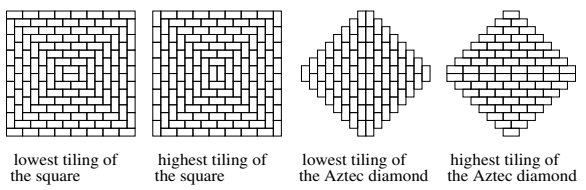

Figure 2: The highest and lowest tilings of the square and Aztec diamond

We derive a new height function $\tilde{h}_T$ that will be useful in the description of Levitov blocks [11, 12]. Adjust the height of any point in the center of the long edge of a domino so that it agrees with the height of its two neighbors along the edge of the domino.

This adjustment forces some points to have two heights simultaneously. If we fit a surface to this new height function so that each domino is covered by a piecewise linear surface, we can add *vertical* triangles to connect the dominoes and account for the multiple heights; these triangles are degenerate in our overhead view and appear as slivers. A Levitov block is made from two triangular prisms with square faces that are glued together so that the square faces are misaligned (viewed from the top one sees two horizontal domino tiles, whereas viewed from below one sees two vertical domino tiles, or vice-versa.); see figure 3. If we start with the surface corresponding to the lowest tiling of a region R, $\tilde{h}_{T_L}(R)$, and start placing Levitov blocks on the surface, the upper envelope will correspond to other domino tilings. If $T_1 \preceq T_2$, then we can get from the surface defined by $\tilde{h}_{T_1}(R)$ to the surface $\tilde{h}_{T_2}(R)$ by adding Levitov blocks.

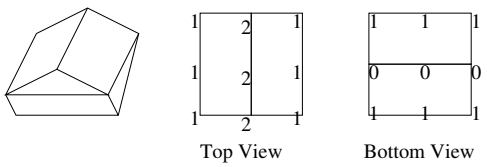

Figure 3: A Levitov tile

3 The model.

The new model consists of filling several families of regions, called *Aztec octahedra* and *tetrahedra*, with prism tiles. We start by defining these tiles and the 3-dimensional regions in section 3.1. The regions are crafted so that the new tilings inherit a height function from the 2-dimensional domino tilings; we define the height function in section 3.2.

3.1 Prism tiles and three-dimensional regions.

The 3-dimensional tiling model consists of a set of identical, prism-shaped tiles and families of 3-dimensional regions, or containers, which are to be perfectly packed with the tiles. Each tile is a triangular prism with $30° \times 30° \times 120°$ triangles and one square face (see figure 4).

We require that in any tiling, square faces of tiles must line up*. When two tiles are misaligned (so that the triangular faces do not form a parallelogram), they look like Levitov blocks. These tiles will always be oriented so that the square base is parallel to the ground, and the projection to the plane below will be two parallel dominoes. When the tiles are aligned, they

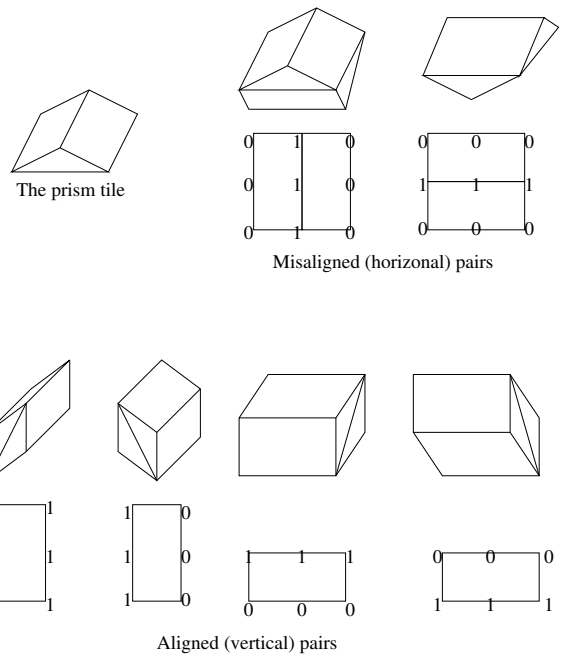

Figure 4: Prism tiles, the possible pairings and their projections

form parallelepipeds. These will always be oriented vertically (so that they have four faces with normals in a plane parallel to the ground) and they project to a single domino (where in the projection the vertical faces are degenerate and align with the boundary of the domino). Figure 4 demonstrates these allowed orientations.

The containers, or regions that we tile, are derived from the 3-dimensional surfaces corresponding to 2-dimensional domino tilings. Given a finite, simply connected region $R \subset \mathbf{Z}^2$, let $V(R) \subset \mathbf{R}^3$ be the region formed by gluing together the surfaces corresponding to the highest and lowest tilings of R. As with Levitov blocks, $V(R)$ is uniquely tileable with prism tiles that must occur in their misaligned orientation. By modifying $V(R)$ we can form more interesting regions with nontrivial tilings. The first region $V_E(R,h)$ is an *elongated volume* formed by translating the surface corresponding to the highest tiling in the vertical direction and adding a vertical wall of height h *units* joining the two surfaces. A vertical *unit* is defined to be $\sqrt{3}/3$. As we will see, when $h = 1$ the set of prism tiles forms a bijection with the set of domino tilings of R; when $h > 1$, the set of tilings forms a bijection with domino chains $T_1 \preceq T_2 \preceq ... \preceq T_h$, where domino tilings respect the partial order.

The second region $V_S(R,h)$ is a *serrated volume* that adds vertical wall of h units in height at *every* level, where levels are horizontal slices distance $\sqrt{3}/3$

*This combinatorial restriction actually is forced by the geometry of the regions being tiled.

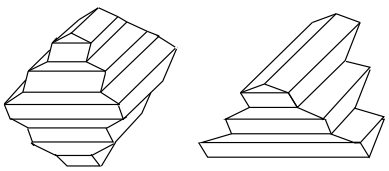

Figure 5: The highest and lowest surfaces arising from the square and Aztec diamond

apart; the horizontal edges on the boundary of $V(R)$ all fall on these slices[†].

If R is the $n \times n$ square, then $V(R)$ is octahedral in shape when n is large. Hence, we call $\mathcal{O}_n = V_E(R,n)$ and $\widehat{\mathcal{O}}_n = V_S(R,1)$ the *Aztec octahedra*. When R is the Aztec diamond of order $n/2$, $V(R)$ is tetrahedral in shape, and we call $\mathcal{T}_n = V_E(R,n)$ and $\widehat{\mathcal{T}}_n = V_S(R,1)$ the *Aztec tetrahedra*. These regions are shown in figure 6.

More precisely, when R is the $n \times n$ square, level i of $V(R)$ is bounded by a $2\lfloor\frac{i+1}{2}\rfloor \times 2\lfloor\frac{i}{2}\rfloor$ rectangle if $1 \le i \le n$ and a $2\lfloor\frac{2n-i}{2}\rfloor \times 2\lfloor\frac{2n-i+1}{2}\rfloor$ rectangle if $n < i \le 2n-1$. From this, we find that level i of $\widehat{\mathcal{O}}_n$ is bounded by a $2\lfloor\frac{i+4}{4}\rfloor \times 2\lfloor\frac{i+2}{4}\rfloor$ if $1 \le i \le 2n-1$ and $2\lfloor\frac{4n-i-1}{4}\rfloor \times 2\lfloor\frac{4n-i+1}{4}\rfloor$ if $2n-1 < i \le 4n-5$.

When R is the Aztec diamond, level i of $V(R)$ is bounded by a $2\lfloor\frac{n-i+2}{2}\rfloor \times 2\lfloor\frac{i}{2}\rfloor$ rectangle, for $1 \le i \le n+1$. Similarly, level i of $\widehat{\mathcal{T}}_n$ is bounded by a $2\lfloor\frac{2n-i+3}{4}\rfloor \times 2\lfloor\frac{i+2}{4}\rfloor$ rectangle, for $1 \le i \le 2n$.

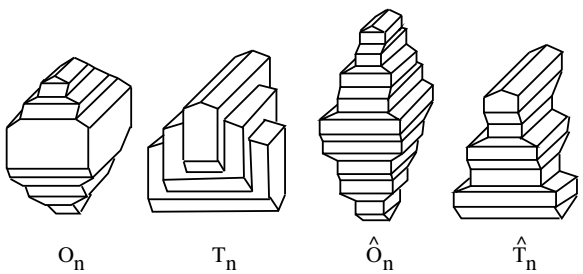

Figure 6: The Aztec octahedra and tetrahedra

3.2 Domino chains and height functions.

For each of the regions defined, the set of prism tilings correspond bijectively to a *domino chain*, a set of h domino tilings $T_1 \preceq T_2 \preceq \ldots \preceq T_h$ that respect the partial order. The vertical walls defined in the construction of the regions are the key to this bijection. We defer rigorous definitions and proofs until the full version of the paper and instead supply intuition behind these correspondences.

The geometry of the shapes forces vertical faces of "aligned" pairs of prisms to be packed along the interior walls of the containers; the transitive closure of the aligned pairs of prisms sharing vertical faces forms a "layer" of vertical tiles. This layer corresponds to one of the domino tilings in the domino chain. We can decompose any prism tiling into a domino chain as follows: Given a tiling of $V_E(R,h)$, we start at the top and remove any misaligned (horizontal) tiles (which are in pairs). The upper envelope of the remaining tiling will consist of aligned (vertical) tiles, which project down to a domino tiling T_h of R. Removing this vertical layer and again removing any horizontal tiles from the top, we reach a second domino tiling T_{h-1} such that $T_{h-1} \preceq T_h$. Continuing in this manner, we find h tilings $T_1 \preceq T_2 \preceq \ldots \preceq T_h$. In fact this map can be shown to be a bijection between 3-dimensional prism tilings of $V_E(R,h)$ and ordered domino tilings.

A bijection holds for tilings of $V_S(R,h)$, but describing this is more complicated because the layers of the 3-dimensional tilings consist of tilings of differently sized subregions of R. To compensate for this, tilings of smaller regions are enhanced with the tiles as they occur in the highest or lowest tiling (depending on whether the layer falls above or below the median layer) to form a complete tiling of R. There is a bijection between prism tilings and sets of domino tilings that satisfy the partial order when they are enhanced in this manner.

These bijections between 3-dimensional prism tilings and domino chains allow us to define a new height function H. Given a prism tiling P corresponding to domino tilings $T_1 \preceq \ldots \preceq T_n$, let $H_P(x,y,i) = h_{T_i}(x,y)$, where $x,y \in \mathbf{Z}^2$ is on the ith level. The set of points $\bigcup_{x,y,i}(x,y,i,H_P(x,y,i))$ describes a surface in $\mathbf{R}^4$. This height function defines a partial order on prism tilings, where $P_1 \preceq P_2$ if $H_{P_1}(x,y,i) \le H_{P_2}(x,y,i)$ for all x,y,i in the region being tiled.

4 Sampling tilings.

To study properties of typical tilings, it is useful to design a Markov chain that connects the state space. In this section we define a Markov chain, where steps consist of rearranging a set of six prism tiles that are packed together. The bijection between prism tilings and domino chains greatly simplifies the description of our Markov chain. Each transition consists of performing a rotation on one of the domino tilings in the domino chain, where moves are only allowed if they continue to respect the partial order. A rotation consists of retiling a 2×2 square on one of the tilings so that

[†]In the definition of the height function, units in the z direction are taken to be $\sqrt{3}/3$ to be consistent with the tiles.

two parallel dominoes are rotated 90° [‡].

We will prove that this Markov chain is rapidly mixing. Our analysis follows the approach taken by Luby, Randall and Sinclair for analyzing a related chain on domino tilings (and other planar configurations) [13].

We first enhance the Markov chain with some non-local moves called "towers" and show that this new Markov chain is rapidly mixing. In the 3-dimensional case the definition of towers is quite sensitive, and it is crucial that we only allow towers within individual domino tilings (and not the z direction) for the argument to work. Showing that the 3-dimensional tower-chain converges quickly requires a careful analysis for which it is useful to reformulate the Luby et. al. proof in terms of path coupling. We do this in section 4.1. In section 4.2 we present the details of the 3-dimensional Markov chain.

4.1 The two-dimensional Markov chain.

We start by reviewing the tower-chain defined and analyzed in [13] for sampling domino tilings in two dimensions. The analysis in [13] is based on a bijection between tilings and *routings*, or sets of nonintersecting lattice paths. It will be useful for us to present an alternative description of the Markov chain in terms of height functions. In addition, the analysis here will use *path coupling* [1], which leads to a somewhat less intuitive proof of the mixing rate, but it will more useful for our generalization to three dimensions in section 4.2.

Elementary domino rotations can be described as follows: pick a point $p \in_u R$, and a sign $s \in_u \{+,-\}$. If p is the center of a 2×2 square filled by two parallel dominoes, and a rotation adjusts the height of p in the direction defined by s, then rotate the dominoes. Otherwise keep the configuration fixed. The tower move enhances this Markov chain with moves involving more dominoes in a "herringbone" arrangement in the NW or SE direction. (See [13] for a more detailed description.) Pick a point $p \in_u R$, a bit $s \in_u \{+,-\}$ and a bit $d \in_u \{NW, SE\}$. If there is a herringbone pattern (or a "tower") starting at p in the d direction such that "rotating" the herringbone adjusts the height of p in the direction defined by s, then (p,s,d) defines a tower of height h, where $h+1$ is the number of dominoes in the herringbone (see figure 7). We choose (p,s,d) with probability $\frac{1}{4N}$, where N is the number of points in the region. Conditioned on choosing these points, the tower is rotated with probability $\frac{1}{h}$. The effect of this move is to increase (or decrease) the height of h points along the "spine" of the tower by ± 4, where the spine is always a zigzag arrangement of points whose heights form an arithmetic progression of difference ± 1. Note that an elementary rotation is now a tower of height 1 in both the NW and SE directions.

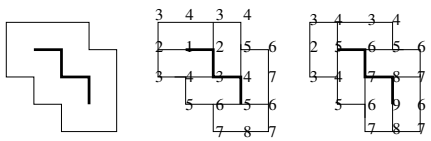

Figure 7: Regions that define domino towers

The transition probabilities $M(\cdot\,,\cdot)$ of $\mathcal{M}_{dom}$ are

$$M(T_1,T_2) = \begin{cases} 1/4Nh, & \text{if } T_1, T_2 \text{ differ by a tower of height } h \\ 1 - \sum_{T \neq T_1} M(T_1,T), & \text{if } T_2 = T_1. \end{cases}$$

The Markov chain $\mathcal{M}_{dom}$ is ergodic and converges to the uniform distribution on tilings. The analysis of the convergence rate relies on a path coupling argument. There is a complete coupling of the state space whereby every configuration is updated simultaneously according to the choice of (p,s,d). We define the distance between two tilings T_1 and T_2 to be $\Phi(T_1,T_2) = \frac{1}{4}\sum_{r \in R}(h_{T_1}(r) - h_{T_2}(r))$, where h_{T_i} is the height function corresponding to T_i (and the factor of $\frac{1}{4}$ accounts for the fact that each domino rotation changes the height of a point by ± 4). This coupling is monotonic so that the partial order on tilings is preserved during coupled updates. The key observation in [13] is that the expected change to Φ in a single move is always at most 0.

LEMMA 4.1. *Let T_1 and T_2 be two domino tilings such that $T_1 \preceq T_2$. Then $\mathrm{E}[\Delta\Phi | T_1, T_2] \leq 0$.*

Proof. Using path coupling [1] and the fact that we have a complete coupling of the state space, it suffices to show that the lemma holds when T_1 and T_2 differ by a single domino rotation, say at the point p. Let $\tau_{r,s,d}$ be the tower starting at r in the direction d if a rotation can be performed in the direction indicated by the sign s. Let $\delta_{r,s,d} = \mathrm{E}[\Delta\Phi | (T_1, T_2, r, s, d)]$ be the expected change to the distance between T_1 and T_2 given the choice of (r,s,d). Then

$$\mathrm{E}[\Delta\Phi | T_1, T_2] = \sum_{r,s,d} \delta_{r,s,d} = \sum_{s,d} \left(\sum_{r} \delta_{r,s,d} \right).$$

Let us assume, without loss of generality, that $s = +$ and $d = NW$. Let q be the neighbor of p to the West

[‡] In terms of the original prism tiling, this move retiles a small region consisting of two pairs of vertical (aligned) tiles and one misaligned pair so that the misaligned pair is moves from above the other tiles to below (or vice-versa).

or North such that $h_{T_i}(q) = h_{T_i}(p)+1 \pmod 4$. We have that

$$\sum_r \delta_{r,+,NW} = \sum_{r\notin\{p,q\}} [\delta_{r,+,NW}] + \delta_{q,+,NW} + \delta_{p,+,NW}.$$

We start with a few key observations (for which we refer the reader to figure 8). The first is that p cannot be in the middle of a spine of a tower in either T_1 or T_2 because the heights of points on a spine must form an arithmetic progression. Similarly, if q is a neighbor of p in the lattice, then q can only be the in the middle of a spine if the tower ends at p. All towers starting at p must have length 1 since both T_1 and T_2 have elementary moves at p. Finally, rotating any tower that does not include p or a neighbor of p on its spine will not cause a change to the distance, since it will be accepted by each configuration in the coupled chain with the same probability.

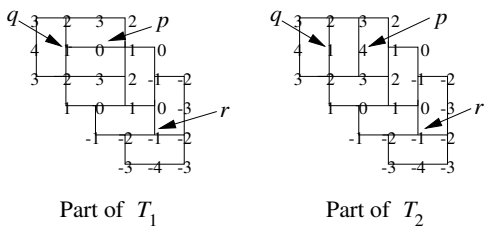

Figure 8: Moves near p in T_1 and T_2.

If we have a NW tower starting at $r \notin \{p,q\}$ that is not identical in T_1 and T_2, it must be that r lies in the SE direction from p. In one configuration $(r,+,NW)$ defines a tower of height h ending at a neighbor of p and in the other configuration it defines a tower of height $h+1$ ending at p. When we couple these moves, with probability $\frac{1}{h+1}$ we will rotate both towers simultaneously, thus decreasing the distance between tilings by 1. With the remaining probability $\frac{1}{h} - \frac{1}{h+1}$ we rotate only the smaller tower, thus increasing the distance by h. The net effect is

$$\delta_{r,s,d} = \frac{1}{h+1}(-1) + \left(\frac{1}{h} - \frac{1}{h+1}\right)(h) = 0,$$

so the expected change to the height function from all points $r \notin \{p,q\}$ is 0. Summarizing this discussion, we have that

$$\begin{aligned}\sum_r \delta_{r,+,NW} &= \delta_{q,+,NW} + \delta_{p,+,NW} \\ &\le \frac{1}{4Nh}(h) + \frac{1}{4N}(-1) = 0,\end{aligned}$$

where h is the height of the tower defined by $(q,+,NW)$, if it exists, since it will add distance h to exactly one tiling. All other choices of s and d are analogous. Hence, $\mathrm{E}[\Delta\Phi|T_1,T_2] = \sum_{s,d}\sum_r \delta_{r,s,d} \le 0$.

We now appeal to theorem 5 of [13]:

LEMMA 4.2. *Suppose there is a coupling which satisfies* $\mathrm{E}\big[\Delta\Phi(t)|X_t,Y_t\big] \le 0$, *and whenever* $\Phi(t) > 0$, $\mathrm{E}\big[(\Delta\Phi(t))^2|X_t,Y_t\big] \ge V$. *Then the expected coupling time from initial states* x,y *satisfies* $\mathrm{E}T^{x,y} \le \Phi(0)\big(2B - \Phi(0)\big)/V$, *where* B *is an upper bound on* Φ.

Following the arguments in [13], we conclude that $\mathcal{M}_{dom}$ is rapidly mixing:

THEOREM 4.1. *Let* R *be a simply connected region of* $\mathbf{Z}^2$. *The mixing time of the Markov chain* $\mathcal{M}_{dom}$ *on domino tilings of* R *satisfies* $\tau(\epsilon) \le \lceil 2\mathrm{e}N^4 \ln\epsilon^{-1}\rceil$, *where* N *is the area of* R.

4.2 A rapidly mixing Markov chain on three-dimensional tilings.

The machinery set up in the last section facilitates the definitions and analysis of a Markov chain for sampling 3-dimensional prism tilings. We are given a region whose domino chain consists of 2-dimensional tilings of regions $R_1,...,R_k$, where the total area is N. The Markov chain consists of tower moves that are restricted to individual tilings in the domino chain.

Each move of $\mathcal{M}_{3dtower}$ is defined by choosing a level $i \in_u \{1,...,k\}$, $p \in_u R_i$, $s \in_u \{+,-\}$ and $d \in_u \{NW,SE\}$. If the point p defines a tower in the direction d in level i such that the height of p changes by 4 according to the sign s, then we choose that tower with probability $\frac{1}{4N}$ and the tower is then rotated with probability $\frac{1}{h}$ (if the resulting configuration is a valid prism tiling). As before, it must be that this rotation leads to a valid domino tiling in the ith level. But now we also have to be careful that levels still respect the partial order. This final restriction blocks moves on level i because of the local configurations on levels $i-1$ and levels $i+1$.

The transition probabilities $M(\cdot,\cdot)$ of $\mathcal{M}_{3dtower}$ are

$$M(P_1,P_2) = \begin{cases} 1/4Nh, & \text{if } P_1 \text{ and } P_2 \text{ differ by a tower of ht } h \text{ in one layer} \\ 1 - \sum_{P\neq P_1} M(P_1,P), & \text{if } P_2 = P_1. \end{cases}$$

As in the 2-dimensional case, this Markov chain is ergodic and converges to the uniform distribution on tilings. We bound the convergence rate by using a monotone complete coupling of the state space. We define the distance between two configurations to be the

sum of the distances between corresponding levels (as defined in section 4.1). Define the distance between two tilings P_1 and P_2 to be $\Phi(P_1, P_2) = \frac{1}{4}\sum_{i,q} |H_{P_1}(q,i) - H_{P_2}(q,i)|$. Again, our task is going to be showing that given two configurations P_1 and P_2, the expected change to the distance is at most 0.

LEMMA 4.3. *Let P_1 and P_2 be two prism tilings such that $P_1 \preceq P_2$. Then $\mathrm{E}[\Delta\Phi|P_1, P_2] \leq 0$.*

Proof. Appealing to path coupling, it suffices to show that the the lemma is true for tilings P_1 and P_2 at distance 1, so they differ by a single domino rotation on a single level, say level i. Thus, if P_1 corresponds to tilings $T_1 \preceq ... \preceq T_i \preceq ... \preceq T_n$, then P_2 corresponds to tilings $T_1 \preceq ... \preceq T_i' \preceq ... \preceq T_n$.

Let $\tau_{j,r,s,d}$ be the tower starting at r in level j in the direction d if a rotation can be performed in the direction indicated by the sign s in either P_1 or P_2. Also, let $\delta_{j,r,s,d} = \mathrm{E}[\Delta\Phi|(P_1, P_2, j, r, s, d)]$ be the expected change to the distance between P_1 and P_2 given the choice of (j, r, s, d). Then

$$\mathrm{E}[\Delta\Phi|P_1, P_2] \;=\; \sum_{j,r,s,d} \delta_{j,r,s,d}.$$

Notice that the only towers which cause a change in the distance between tilings must be on level $i-1, i$ or $i+1$. Hence, restricting to levels $i-1$, i and $i+1$ and regrouping terms in an unusual, but useful way, we find:

$$\mathrm{E}[\Delta\Phi|P_1, P_2] = \sum_{s,d}\Big[\sum_r \delta_{i,r,s,d} + \sum_r \delta_{i-1,r,-s,-d} + \sum_r \delta_{i+1,r,-s,-d}\Big],$$

where $-s$ and $-d$ reverse the sign and direction. Let us assume, without loss of generality, that $s = +$ and $d = NW$. Let q be the unique neighbor of p to the West or North on level i such that $h_{T_i}(q) = h_{T_i}(p) - 1 \ (mod\ 4)$. Again, the only towers in the ith level which cause a change to the distance between tilings must start at p, q or a point r to the SE of p. Any tower starting at r that is allowable must have height h in one configuration and height $h+1$ in the other, and the net effect of choosing r will be 0. This gives us that

$$\begin{aligned}\sum_r \delta_{i,r,+,NW} + \sum_r \delta_{i-1,r,-,SE} + \sum_r \delta_{i+1,r,-,SE} \\ = \delta_{i,q,+,NW} + \delta_{i,p,+,NW} + \sum_r \delta_{i-1,r,-,SE} \\ + \sum_r \delta_{i+1,r,-,SE}.\end{aligned} \tag{4.1}$$

Now note that $\sum_r \delta_{i-1,r,-,SE} = 0$ since any move that tries to decrease the height of some points on level $(i-1)$ will not be affected by the difference on the ith level. If there is a tower on level $i+1$ that can only be rotated in one of the tilings, it must be that it starts at p (because the fact that it is blocked in one of the tilings indicates that p is a local minimum on level $i+1$). All other tower moves are either accepted (or rejected) in both tilings. Hence, equation 4.1 is just

$$\delta_{i,q,+,NW} + \delta_{i,p,+,NW} + \delta_{i+1,p,-,SE}.$$

We know that $\delta_{i,p,+,NW} < 0$, so it suffices to show that $\delta_{i,q,+,NW} + \delta_{i+1,p,-,SE}$ cannot be too large. A case analysis reveals that either $\delta_{i,q,+,NW} = 0$ or $\delta_{i+1,p,-,SE} = 0$ as follows. Suppose $\delta_{i+1,p,-,SE} > 0$. Then for $\tau_{i+1,p,-,SE}$ to be a tower in *exactly one* tiling, it must be that $H_{P_1}(q, i+1) = H_{P_1}(q, i)$ (recall these heights are the same in P_1 and P_2). But then $\tau_{i,q,+,NW}$ must be blocked. Therefore at most one of $(i+1, p, -, SE)$ and $(i, q, +, NW)$ can define a tower. As in the 2-dimensional case, the expected change due to any single move is at most $1/4N$, hence

$$\delta_{i,q,+,NW} + \delta_{i+1,p,-,SE} \leq \frac{1}{4N}.$$

Therefore,

$$\begin{aligned}&E[\Delta\Phi|P_1, P_2, +, NW] \\ &\quad = \delta_{i,q,+,NW} + \delta_{i,p,+,NW} + \delta_{i+1,p,-,SE} \leq 0.\end{aligned}$$

All other choices of (s, d) are analogous, so

$$\mathrm{E}[\Delta\Phi|T_1, T_2] = \sum_{i,r,s,d} \delta_{i,r,s,d} \leq 0.$$

Appealing again to lemma 4.2 (theorem 5 of [13]), we conclude that $\mathcal{M}_{3dtower}$ is rapidly mixing.

THEOREM 4.2. *Let R be a region which can be tiled with layered prism tiles. The mixing time of the Markov chain $\mathcal{M}_{3dtower}$ on tilings of R satisfies $\tau(\epsilon) \leq \lceil 2eN^4 \ln \epsilon^{-1} \rceil$, where N is the volume of R.*

We conclude this section by returning to the original description of the Markov chain where transitions are restricted to be elementary domino rotations (and not tower moves). The comparison method of Diaconis and Saloff-Coste [4] can be used to show that the rapid convergence of $\mathcal{M}_{3dtower}$ implies the rapid mixing of this simpler Markov chain. This analysis follows the argument given by Randall and Tetali in the 2-dimensional case [15].

5 Properties of random tilings.

Using the technology set forth in section 4, it is possible to uniformly sample tilings. We conjecture that the elongated volumes have frozen regions akin to the arctic circle theorem in two dimensions. Random tilings of the serrated volumes, on the other hand, do not have predictably tiled subregions. We show, in fact, that the entropy of $\widehat{\mathcal{O}}$ is equal to the entropy of $\widehat{\mathcal{T}}$. The proof suggests that the local statistics of the tilings will be uniform throughout these regions. We present this proof in section 5.1. In section 5.2 we show random tilings of the elongated volumes which were generated using the Markov chain.

5.1 The entropy of serrated volumes $\widehat{\mathcal{O}}$ and $\widehat{\mathcal{T}}$.

The *entropy* of a physical system captures many of its thermodynamic properties; intuitively it conveys information about the average "randomness" captured by typical configurations. More precisely, the entropy S of a family of regions $\mathcal{R} = \{R_n\}$ is defined as $S = \lim_{n\to\infty} \frac{\log \#(R_n)}{\mathrm{Vol(R_n)}}$, where $\#(R_n)$ is the number of tilings of region R_n. In this section we show that tilings of the Aztec tetrahedron $\widehat{\mathcal{T}}_n$ and the Aztec octahedron $\widehat{\mathcal{O}}_n$ have equal entropy when n is large.

Let $\#(R)$ be the number of tilings of a region R. We let $a_n = \log \#(\widehat{\mathcal{O}}_n)$, $A_n = \mathrm{Vol}(\widehat{\mathcal{O}}_n)$ be the volume, and let $\alpha_n = \frac{a_n}{A_n}$ be their ratio. Similarly, we let $b_n = \log \#(\widehat{\mathcal{T}}_n)$, $B_n = \mathrm{Vol}(\widehat{\mathcal{T}}_n)$ and $\beta_n = \frac{b_n}{B_n}$. The goal of this section is to show that $\lim_{n\to\infty} \alpha_n = \lim_{n\to\infty} \beta_n$, thus implying that the tilings of $\{\widehat{O}_n\}$ and $\{\widehat{T}_n\}$ have equal entropy in the limit.

We start with a few lemmas which show an interesting combinatorial decomposition of the tetrahedral and octahedral regions showing that they can be exactly packed with smaller octahedral and tetrahedral regions. These decompositions are very similar to the well-known decompositions of true octahedra and tetrahedra, with the technical detail that a mixture of tetrahedral regions of size p and $p-1$ must be used to compensate for the irregular boundaries of the Aztec regions we study. The corollaries to these lemmas use these decompositions to show that the logarithms of the number of tilings of these regions satisfy a superadditive relationship. We offer pictorial proof sketches of the lemmas in the special case that $k = 2$ and defer the details for the full version of the paper.

LEMMA 5.1. *The tetrahedral pyramid of order kn, $\widehat{\mathcal{T}}_{kn}$, can be packed with smaller Aztec octahedra and tetrahedra such that:*

$$B_{kn} = c_1 A_n + c_2 B_n + c_3 B_{n-1},$$

where $c_1 = \frac{k^3-k}{6}, c_2 = \frac{k^3+3k^2+2k}{6}$ *and* $c_3 = \frac{k^3-3k^2+2k}{6}$.

When $k = 2$, lemma 5.1 says $B_{2n} = A_n + 4B_n$. In other words, an Aztec tetrahedron of size $2n$ can be exactly packed with one Aztec octahedron and four Aztec tetrahedra of size n. To demonstrate this decomposition in this special case, we refer the reader to figure 9. The leftmost picture represnts the lowest tiling an Aztec diamond, which corresponds to the view from above of an empty Aztec tetrahedron of order $2n$. The next picture represents the tiling corresponding to the Aztec tetrahedron after two small tetrahedra of order n are packed inside. Finally, after adding an octahedron and 4 tetrahedra, we arrive at the rightmost picture, which corresponds to the highest tiling of the Aztec diamond (and the volume is fully packed).

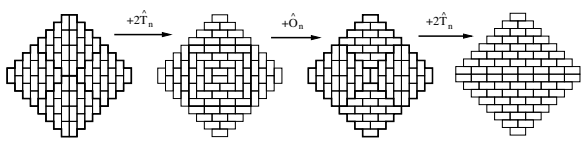

Figure 9: The proof of lemma 5.1 when $k = 2$.

COROLLARY 5.1. *The logarithm of the number of tilings of $\widehat{\mathcal{T}}_n$ satisfies $b_{kn} \geq c_1 a_n + c_2 b_n + c_3 b_{n-1}$.*

We find a similar decomposition for $\widehat{\mathcal{O}}_n$:

LEMMA 5.2. *The octahedral pyramid of order kn, $\widehat{\mathcal{O}}_{kn}$, can be packed with smaller Aztec octahedra and tetrahedra such that:*

$$A_{kn} = c_4 A_n + c_5 (B_n + B_{n-1}),$$

where $c_4 = \frac{2k^3+k}{3}$ *and* $c_5 = \frac{2k^3-2k}{3}$.

When $k = 2$, lemma 5.2 states $A_{2n} = 6A_n + 4B_n + 4B_{n-1}$. Again, we demonstrate this proof pictorially in this special case (see figure 10).

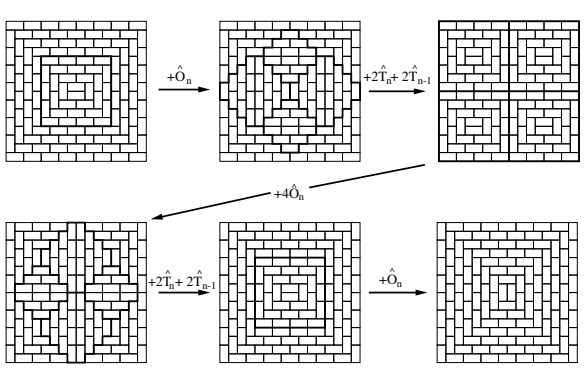

Figure 10: The proof of lemma 5.2 when $k = 2$.

COROLLARY 5.2. *The logarithm of the number of tilings of* $\widehat{\mathcal{O}}_n$ *satisfies* $a_{kn} \geq c_4 a_n + c_5\,(b_n + b_{n-1})$.

We use these calculations to show that the entropy of the two families of regions turns out to be the same. The superadditive lemmas 5.1 and 5.2 allow us to upper bound the entropy of each region in terms of the other, thus establishing equality.

THEOREM 5.1. *The entropy of tilings of the Octahedral pyramid* $\widehat{\mathcal{O}}_n$ *and the Tetrahedral pyramid* $\widehat{\mathcal{T}}_n$ *are equal:*

$$\lim_{n\to\infty} \alpha_n = \lim_{n\to\infty} \beta_n.$$

Proof. Fix n and p, and let $k = \lfloor \frac{n-1}{p} \rfloor$ and $r_1 = \frac{A_{kp}}{A_n} < 1$ be the ratio of the volumes of two closely related regions. Then

$$\begin{aligned}
\alpha_n &= \frac{a_n}{A_n} \\
&\geq r_1\, \frac{a_{kp}}{A_{kp}} \\
&\geq r_1\, \frac{c_4 a_p + c_5\,(b_p + b_{p-1})}{A_{kp}} \\
&= \frac{r_1}{A_{kp}} \left(c_4 A_p \frac{a_p}{A_p} + c_5 B_p \frac{b_p}{B_p} + c_5 B_{p-1} \frac{b_{p-1}}{B_{p-1}} \right)
\end{aligned}$$

where $c_4 = (2k^3 + k)/3$ and $c_5 = (2k^3 - 2k)/3$ are from the statement of corollary 5.2.

Now, letting $Min_p = \min(\alpha_p, \beta_p, \beta_{p-1})$, and using the volume relationships from lemma 5.2, it follows that

$$\begin{aligned}
\alpha_n &\geq r_1\ Min_p \frac{c_4 A_p + c_5 B_p + c_5 B_{p-1}}{A_{kp}} \\
&= r_1\ Min_p .
\end{aligned}$$

As $n \to \infty$,

$$\underline{\lim}\, \alpha_n \geq \underline{\lim}\ r_1\ Min_p = Min_p .$$

This holds for all p, so

$$\underline{\lim}\, \alpha_n \geq \sup\ Min_p . \tag{5.1}$$

We now use the tetrahedral decompositions to achieve a similar bound on $\underline{\lim}\, \beta_n$. Letting $r_2 = \frac{B_{kp}}{B_n}$, the analogous calculations yield

$$\beta_n \geq r_2\ Min_p .$$

Thus,

$$\underline{\lim}\, \beta_n \geq \sup\ Min_p . \tag{5.2}$$

In addition, since we chose k to be $\lfloor \frac{n-1}{p} \rfloor$, we have, by an identical argument,

$$\underline{\lim}\, \beta_{n-1} \geq \sup\ Min_p . \tag{5.3}$$

Putting together inequalities 5.1, 5.2 and 5.3, we have that

$$\underline{\lim}\ Min_n \geq \sup\ Min_p .$$

Hence, since $\sup\ Min_n \geq \overline{\lim}\, Min_n$, it follows that $\lim\ Min_n$ exists and

$$\lim\ Min_n = \sup\ Min_n . \tag{5.4}$$

To complete the proof, we need to argue that $\lim \alpha_n = \lim \beta_n$. Let $Max_p = \max(\alpha_p, \beta_p, \beta_{p-1})$. It suffices to show that $\lim\ Max_n = \lim\ Min_n$. Again, fix p and let $k = \lfloor \frac{n-1}{p} \rfloor$. From lemma 5.1 and 5.2, we have that

$$\alpha_n \geq \frac{c_1 A_p}{A_n}\alpha_p + \frac{c_2 B_p}{A_n}\beta_p + \frac{c_3 B_{p-1}}{A_n}\beta_{p-1},$$

and

$$\min(\beta_n, \beta_{n-1}) \geq \frac{c_4 A_p}{B_n}\alpha_p + \frac{c_5 B_p}{B_n}\beta_p + \frac{c_5 B_{p-1}}{B_n}\beta_{p-1}.$$

Therefore, letting

$$\hat{c}_n = \min\left(\frac{c_1 A_p}{A_n}, \frac{c_2 B_p}{A_n}, \frac{c_3 B_{p-1}}{A_n}, \frac{c_4 A_p}{B_n}, \frac{c_5 B_p}{B_n}, \frac{c_5 B_{p-1}}{B_n} \right),$$

we see that

$$Min_n \geq \hat{c}_n(\ Max_p - \ Min_p) + \ Min_p .$$

If $p > 4$, then a simple calculation determining the ratio of volumes reveals that $\hat{c} \geq 1/6$. Since $\lim \hat{c}_n$ is bounded away from zero, the equality in equation 5.4 implies that $\lim\ Max_n = \lim\ Min_n$. Consequently,

$$\lim \alpha_n = \lim \beta_n .$$

5.2 Frozen regions in elongated volumes.
Our simulations demonstrate that the elongated volumes behave quite differently than the serrated volumes. It appears that $\mathcal{O}_n$ and $\mathcal{T}_n$ have bounded regions, outside of which the tilings appear frozen. Figures 11 and 12 demonstrate this phenomenon (frozen regions are omitted). We call the boundary of the frozen region of $\mathcal{O}_n$ the "arctic sphere" and conjecture that the arctic sphere converges to a true sphere (slightly truncated by the vertical walls).

Acknowledgements.
We are grateful to Russell Martin for many helpful comments on this paper. The first author would also like to thank Jim Propp for demonstrating the connection between height functions and Levitov tiles.

Figure 11: Random tiling of an Aztec octahedron.

Figure 12: Random tiling of an Aztec tetrahedron.

References.

[1] Bubley, R. and Dyer, M. Path coupling: A technique for proving rapid mixing in Markov chains. *38th IEEE Symposium on Foundations of Computer Science* 1997.

[2] Ciucu, M. An improved upper bound for the three dimensional dimer problem. *Duke Math. J.* **94** (1998), pp. 1-11.

[3] Conway, J. and Lagarias, J. Tilings with polyominoes and combinatorial group theory. *Journal of Combinatorial Theory A* **53** (1990), pp. 183–208.

[4] Diaconis, P. and Saloff-Coste, L. Comparison theorems for reversible Markov chains. *Ann. Appl. Probability* **3** (1993), pp. 696–730.

[5] Elkies, N., Kuperberg, G., Larsen, M. and Propp, J. Alternating-Sign Matrices and Domino Tilings. *Journal of Algebraic Combinatorics* **1** (1992), pp. 111-132 and 219-234.

[6] Fowler, R.H. and Rushbrooke, G.S. Statistical theory of perfect solutions. *Transactions of the Faraday Society* **33**, (1937), pp. 1272-1294.

[7] Heilmann, O.J. and Lieb, E.H. Theory of monomer-dimer systems. *Communications in Mathematical Physics* **25** (1972), pp. 190–232.

[8] Jockusch, W., Propp, J. and Shor, P. *Random domino tilings and the arctic circle theorem.* Eprint: math.co/9801068 (1995).

[9] Kasteleyn, P.W. The statistics of dimers on a lattice I. The number of dimer arrangements on a quadratic lattice. *Physica* **27** (1961), pp. 1209–1225.

[10] Kenyon, C., Randall, D. and Sinclair, A. Approximating the number of dimer coverings of a lattice. *Journal of Statistical Physics* **83** (1996), pp. 637–659.

[11] Levitov, L. S. The RVB model as the problem of the surface of a quantum crystal. *JETP Letters* **50** (1989), pp. 469-472.

[12] Levitov, L. S. Equivalence of the dimer resonance-valence-bond problem to the quantum roughening problem. *Phys. Rev. Letters* **64** (1990), pp. 92-94.

[13] Luby, M., Randall, D. and Sinclair, A. Markov chain algorithms for planar lattice structures. *Proc. 36th IEEE Symposium on Foundations of Computing* (1995), pp. 150-159.

[14] Luby, M., Randall, D. and Sinclair, A. Markov chain algorithms for planar lattice structures. Preprint, 1999.

[15] Randall, D. and Tetali, P. Analyzing Glauber dynamics by comparisons of Markov chains. *Proc. 3rd Latin American Theoretical Informatics Symposium,* Springer Lecture Notes in Computer Science Vol. **1380** (1998), pp. 292-304.

[16] Temperley, H.N.V. and Fisher, M.E. Dimer problem in statistical mechanics–an exact result. *Philosophical Magazine* **6** (1961), pp. 1061–1063.

[17] Thurston, W. Conway's tiling groups. *American Mathematical Monthly* **97** (1990), pp. 757–773.